

# Three-body recombination at vanishing scattering lengths in an ultracold Bose gas

Zav Shotan<sup>1\*</sup>, Olga Machtey<sup>1\*</sup>, Servaas Kokkelmans<sup>2</sup>, and Lev Khaykovich<sup>1</sup>

<sup>1</sup>*Department of Physics, Bar-Ilan University, Ramat-Gan, 52900 Israel and*

<sup>2</sup>*Eindhoven University of Technology, P.O. Box 513, 5600 MB Eindhoven, The Netherlands*

(Dated: April 24, 2019)

We report on measurements of three-body recombination rates in an ultracold gas of  $^7\text{Li}$  atoms in the extremely non-universal regime where the two-body scattering length vanishes. We show that the rate is well-defined and can be described by two-body parameters only: the scattering length  $a$  and the effective range  $R_e$ . We find the rate to be energy-independent, and by connecting our results with previously reported measurements in the universal limit we cover three-body recombination in the whole range from weak to strong two-body interactions. We identify a non-trivial magnetic field value in the non-universal regime where the rate should be strongly reduced.

PACS numbers: 34.50.Cx, 21.45.-v, 67.85.-d

The few-body problem underlies fundamental processes in physics, yet it is notoriously difficult for finding analytic and numerical solutions [1]. It challenges our mind with the complexity of small and system-dependent molecular structures at the size of their interaction potentials. At the same time, in the regime of resonant pairwise interactions, it provides an elegant description of unusually large bound states possessing universal properties. Two important two-body length scales are involved in this description. The first is the van der Waals length  $r_{\text{vdW}}$ , which is constant and connected to the radial range of the potential. The second is the  $s$ -wave scattering length  $a$ , which can be tuned magnetically via a Feshbach resonance [2]. When  $a \gg r_{\text{vdW}}$ , universal two-body states with size  $\sim a$  emerge, and a wealth of phenomena known as Efimov physics is opened up in three- and, generally,  $N$ -body sectors [3, 4]. The fundamental states belonging to the Efimov effect (Efimov trimers) depend log-periodically on  $a/r_{\text{vdW}}$  [5, 6].

Sufficiency of two-body parameters in the Efimov scenario indicates that two-body physics plays a decisive role in the universal few-body processes in ultracold gases. The following questions raise on how far this dominance of two-body physics extends when going to the opposite, non-universal limit, *i.e.* when  $a \rightarrow 0$ . What parameters govern the three-body processes and can we identify the influence of the short-range three-body forces in this limit? Although recent theoretical studies probe the non-universal regime [7–9], their approaches cannot be directly extended to the regions of extreme non-universality, the scattering length zero-crossings.

Three-body recombination has been extensively used as an efficient probe of Efimov physics in trapped ultracold gases [10–16]. The process involves collisions of three particles resulting in a formation of a two-body bound state and a free atom. The binding energy, usually much larger than the trap depth, is then released as kinetic energy of the colliding partners inducing inelastic losses.

In this Letter, we investigate three-body recombination rates in the vicinity of two different zero-crossings in a gas of ultracold  $^7\text{Li}$  atoms. One zero-crossing is associated with a broad Feshbach resonance, while the other one is connected to a narrow resonance. We demonstrate a clear difference between the two regions with  $a \approx 0$ , and explain the magnetic field dependence of the three-body recombination rate in terms of a new effective length parameter. This parameter describes the two-body scattering phase shift for vanishing scattering length, and can be understood in terms of the finite range of the two-body potential, given by the van der Waals length, and by the width of the Feshbach resonance.

Assuming the dominance of the two-body physics in three-body processes, we start by considering the effective range expansion of the scattering phase shift  $\delta(k)$  in its usual form [17]:

$$k \cot \delta(k) = -\frac{1}{a} + \frac{R_e k^2}{2}. \quad (1)$$

However, when  $a \rightarrow 0$  the first term diverges and to compensate this divergence the second term diverges as well ( $|R_e| \rightarrow \infty$ ), which makes the above expression inconvenient in this limit. A better form of the effective range expansion can be obtained by revamping the standard expression as:

$$-\frac{\tan \delta(k)}{k} = a - V_e k^2, \quad (2)$$

where  $V_e = -R_e a^2/2$  is the effective volume. We show that although neither  $a$  nor  $R_e$  are good lengths at zero-crossings, their combination in the form of the effective length  $L_e = V_e^{1/3}$  remains finite, and captures remarkably well the behaviour of the three-body recombination rate [27]. Once  $a$  and  $L_e$  are known, no further knowledge of the short-range two-body or three-body potentials is needed. Moreover, while the two-body collisional cross-section becomes energy dependent at a zero-crossing, the three-body recombination rate remains energy independent. In addition we show that  $L_e$  continues to be the dominate length in the inelastic three-body processes for

---

\*These authors contributed equally to this work

larger scattering lengths up to a region where the universal three-body physics takes over and the leading length becomes  $a$ .

In the experiment we use an ultracold sample of  $^7\text{Li}$  atoms prepared in the  $|F = 1, m_F = 0\rangle$  state, where two Feshbach resonances allow for tunability of the scattering length  $a$ . The first resonance is located at 845.5G and is closed-channel dominated, the second resonance is located at 894G, and is in between being closed- and open-channel dominated. These resonances were precisely located and characterized in Ref. [18] by fitting the binding energies of weakly bound dimers obtained in rf-association spectroscopy with coupled channel calculations. Fig. 1(a),(b) shows  $a$  (green solid line) and  $R_e$  (blue dashed-dotted line) dependence on the external magnetic field  $B$  from our most up-to-date coupled channels analysis [18]. Divergences of the scattering length correspond to the resonance positions. In Ref. [19] a log-periodic behaviour of the three-body recombination rate coefficient has been demonstrated in the vicinity of the 894G resonance in the limit of  $a \gg r_{\text{vdW}}$ . Here, in contrary, we are interested in regions where the scattering length crosses zero. In Fig. 1 two zero-crossings are shown: at 850.1G and 575.9G. We ignore the third zero-crossing at  $\sim 412\text{G}$  (not shown in the figure) for its apparent similarity to one at 575.9G from the present studies point of view. As was noted earlier,  $R_e$  diverges at zero-crossing which can be seen in Fig. 1(a).

First, we consider two-body elastic processes for the 850.1G zero-crossing. From Eq. (2) we obtain the energy-dependent s-wave collisional cross-section between two identical bosons:

$$\sigma(k) = \frac{8\pi}{k^2} \sin^2(\delta(k)) = \frac{8\pi (V_e k^2 - a)^2}{1 + (V_e k^2 - a)^2 k^2}. \quad (3)$$

Accordingly,  $\sigma(k)$  vanishes when  $a = V_e k^2$ , reflecting the emergent energy dependence of the two-body collisional cross-section.

Elastic collisions are crucial for evaporative cooling, therefore the absence of cooling serves as the experimental strategy to find a vanishing cross section  $\sigma(k) = 0$ . In the experiment,  $^7\text{Li}$  atoms are trapped in a crossed beam optical dipole trap [20] and we perform a fast cooling at the last stage of the evaporation cycle by lowering the power of the laser beams in 500 ms at different magnetic fields. The initial temperature of atoms is measured to be  $31.1(1.1)\mu\text{K}$  and the final temperature as a function of  $B$  is represented in Fig. 2. A maximum in temperature can be clearly identified at 850.4G which indicates the total failure of the evaporation cooling routine. We model the temperature decrease during evaporation with the set of two coupled rate equations: for number of atoms  $N$  and temperature  $T$  [28]. The model includes the time evolution of temperature due to evaporation cooling which vanishes when  $\sigma(k) = 0$  and adiabatic cooling due to weakening of the optical dipole potential [21]. The latter, being a single-body effect, is independent of  $\sigma(k)$  and works equally well for all magnetic field values. The

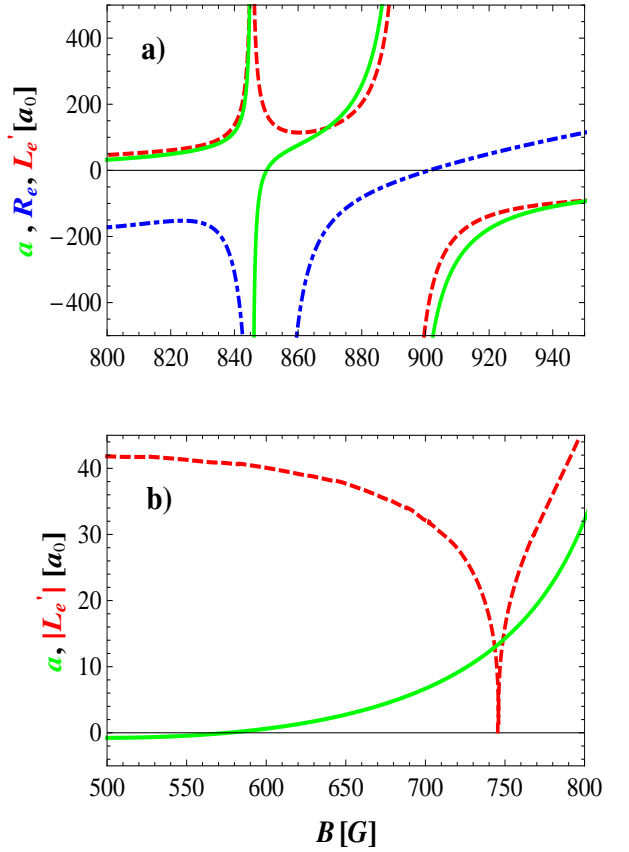


FIG. 1: Scattering length  $a$  (green solid line), effective range  $R_e$  (blue dashed-dotted line) and effective length  $L'_e$  (red dashed line) as a function of the magnetic field  $B$ . (a) - Region of the high field zero-crossing with  $a = 0$  at 850.1G.  $a$  diverges at the positions of Feshbach resonances at 845.5G and 894G.  $R_e$  diverges when  $a \rightarrow 0$ . (b) - Region of the low field zero-crossing with  $a = 0$  at 575.9G. The absolute value of  $L'_e$  is shown to emphasize the  $L'_e = 0$  point at 744.15G, where  $R_e$  (not shown) rapidly changes sign.

solid blue line in Fig. 2 represents the solution to our model with no adjustable parameters. The agreement is remarkable which confirms that the two-body elastic collisional cross-section is consistent with 0 at the magnetic field of 850.4G. This value is shifted from the 850.1G zero-crossing due to the energy dependence of  $\sigma(k)$ . The  $T = 0$  model is represented as a dashed line in the figure and shows poor agreement with the data.

The same experimental strategy can be applied to identify another  $\sigma(k) = 0$  position related to the lower magnetic field zero-crossing. However weak dependence of  $a$  on  $B$  in this region allows for a significant tolerance in the uncertainty of the zero-crossing position. From the current studies point of view, this is also indicated by the very weak magnetic field dependence of the three-body effective length  $L'_e$  (explained below) around 575.9G (see Fig.1(b)).

Now we turn to three-body inelastic processes, however, first it is worth noting that the  $|F = 1, m_F = 0\rangle$

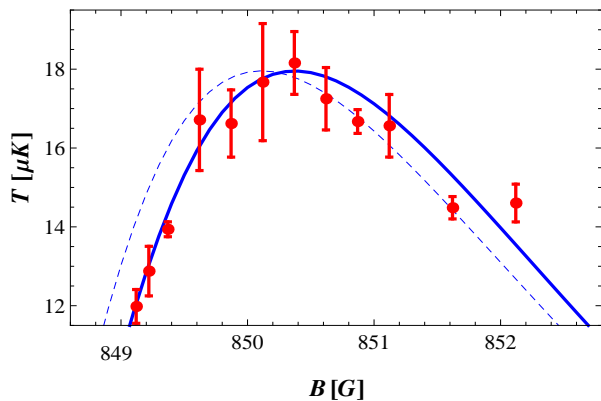


FIG. 2: Temperature at the end of the fast evaporation cycle as a function of the magnetic field  $B$ . Maximal temperature is obtained when  $\sigma(k) = 0$ , corresponding to the total failure of evaporation cooling. The blue solid line is the finite temperature theory model described in text with no adjustable parameters. The dashed line represents the theory model at  $T = 0$  limit which shows poor agreement with data.

state is not the absolute ground state of the system and thus two-body inelastic dipole-dipole relaxation is allowed. However, as shown in Ref. [18] it is extremely weak for all magnetic field values relevant for the present studies, and the dominant inelastic mechanism is induced by three-body recombination.

After loading atoms from a magneto-optical trap into an optical dipole trap we perform evaporative cooling at the wing of the narrow resonance. Then we jump across the resonance to 858G within 1ms and wait for 500ms before we move within 10ms to the target field where the atom number and temperature evolutions are measured. The typical holding time at the final magnetic field varies between 5 to 20 sec where we lose  $\sim 50\%$  of the atoms. The three-body recombination loss rate coefficient  $K_3$  is extracted from the fit of the atom number decay with the solution to the three-body loss rate differential equation:  $\dot{N} = -K_3 \langle n^2 \rangle N - \Gamma N$ , where  $\Gamma$  is the single-body loss rate coefficient due to residual collisions with thermal atoms in the vacuum. Three-body recombination is known to be accompanied by heating and the  $K_3$  coefficient should be extracted from a set of two coupled rate equations: atom number and temperature time evolutions [22]. Even with this precaution, the  $K_3$  coefficient usually deviates from theoretically predicted  $a^4$  dependence in the universal regime [3] which can be attributed mainly to the uncertainties in the atom number calibration. An elegant method to calibrate atom number is based on the equation of state measurements recently used to characterize the unitary regime where  $|a| \rightarrow \infty$  [12]. Here we use the amplitude factor for  $K_3$  coefficient previously determined in our system in the universal regime to calibrate our data [18, 19, 23]. We emphasize that the same factor is used to calculate the theory curve of the two-body elastic collisions in Fig. 2. Excellent agreement between the theory and the exper-

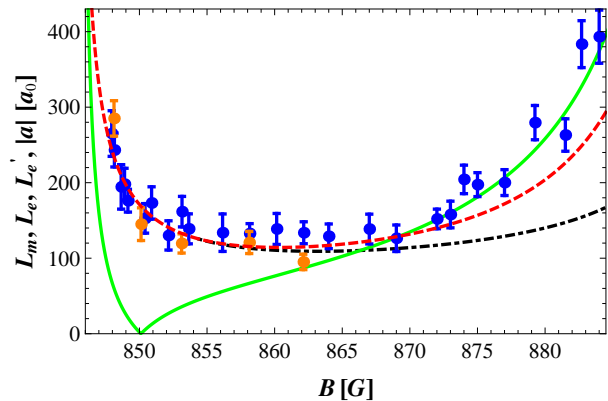


FIG. 3: Measurements of the three-body recombination length  $L_m$  at  $2.5\mu\text{K}$  (blue dots) and  $10\mu\text{K}$  (orange dots). Black dashed-dotted line represents the effective recombination length  $L_e$  and red dashed line shows the modified effective length  $L'_e$  that includes  $a^3$  term correction (see Eq. 6). Green solid line represents the modulus of the scattering length  $|a|$ .

imental results represented in both Figs. 2 and 3 (explained below) hints at the correct interpretation of the amplitude factor. Note also that as we do not study extreme variations in three-body recombinations, temperature dynamics is similar at different magnetic fields. Thus using a single rate equation for atom number decay to extract  $K_3$  coefficient causes only a slight correction to the overall amplitude factor.

For  $a \gg r_{\text{vdW}}$  the three-body recombination loss rate coefficient  $K_3$  is represented as  $K_3 = 3C(a)\hbar a^4/m$ . The general  $a^4$  power dependence is dictated by the resonantly enhanced two-body interactions, while  $C(a)$  reflects the discrete scaling invariance of  $K_3$  related to Efimov physics [3]. For positive scattering length,  $C(a)$  includes oscillations on log scale with the maximum value of  $\sim 70$ . Due to relatively short lifetime of Efimov trimers in  $^7\text{Li}$  (large inelastic parameter  $\eta_*$ ), this value was measured to be somewhat smaller,  $\sim 54.7$  [19].

The universal  $a^4$  dependence is expected to break down when  $a \rightarrow 0$ . Still we can formally represent the three-body recombination coefficient as

$$K_3 = 3C \frac{\hbar}{m} L_m^4 \quad (4)$$

with  $L_m$  being a characteristic recombination length for the measured  $K_3$  values and  $C$  is assumed to be a scattering length independent constant. The results of  $L_m$  as a function of the magnetic field  $B$  for two different temperatures are shown in Fig. 3 (blue and orange dots) setting  $C = 54.7$ , the universal limit's maximal value. Above  $\sim 865\text{G}$  we reproduce the measurements from Ref. [19] where  $L_m$  follows  $a$  (green solid line). For lower values of the magnetic field, deviations from the  $a$ -dependence become evident. Instead of decreasing with  $a$ ,  $L_m$  saturates at  $\sim 120a_0$  where  $a_0$  is the Bohr radius and starts to increase again below  $\sim 855\text{G}$ . Nothing dramatic happens at the point of the scattering length's zero-crossing

where  $L_m$  continues to increase smoothly.

To analyze the data we assume that the two-body physics plays a decisive role in three-body recombination rates, and that the relevant parameter can be directly extracted from the expansion of the two-body phase shift:

$$\delta(k) = -ka + V_e k^3 + \frac{k^3 a^3}{3}. \quad (5)$$

When  $a \rightarrow 0$ , the dominant term in Eq. (5) is  $(L_e k)^3$  where the effective length is  $L_e = (-R_e a^2/2)^{1/3}$ .  $L_e$  is represented in Fig. 3 as a black dashed-dotted line. It stays finite for vanishing  $a$  and diverging  $R_e$ . Moreover, in the vicinity of 850.1G it agrees remarkably well with the data with no adjustable parameters. This agreement confirms our assumption that the two-body physics alone defines the behaviour of  $K_3$ . For larger magnetic field values,  $L_e$  starts to slightly deviate from the data. However, according to Eq. (5), for larger scattering length the two-body scattering volume should be appended by the  $a^3$  term and the effective length then becomes:

$$L'_e = \left( \frac{a^3}{3} - \frac{R_e a^2}{2} \right)^{1/3}. \quad (6)$$

In Fig. 3  $L'_e$  is shown as a red dashed line (indistinguishable from the black line below 855G) and it is in excellent agreement with the data up to 870G at which the first term in Eq. (5) becomes dominant.

Note that for two-body elastic scattering in the  $a \rightarrow 0$  limit, the effective volume  $V_e$  is multiplied by  $k^2$  (see Eq. (3)) to form the effective collisional length which is then explicitly energy dependent. In contrary,  $L_e$  and  $L'_e$  possess no explicit energy dependence. As the relevant length for the three-body recombination rate can be constructed differently as compared to Eq. (6), *e.g.* as the aforementioned effective collisional length, the question of energy dependence of  $K_3$  remains open. We thus measure the three-body recombination rate at a different temperature, 10 $\mu$ K, and the result is shown in Fig. 3 (orange dots). The two measurements are indistinguishable within the experimental errors providing an evidence that  $K_3$  is energy independent. As an additional argument we note that if  $L'_e$  is defined according to Eq. (6), the measured recombination length  $L_m$  agrees with it if  $C$  in Eq. (4) is set to 54.7, the same value as in the universal limit where  $a \gg r_{\text{vdW}}$ . Any attempt to plug-in the energy dependence in  $L'_e$  will require tuning of  $C$  to a significantly different value.

Finally, we consider the zero-crossing at 575.9G. If we assume again  $L_e$  to be the relevant length there, then

the three-body recombination rate can be evaluated from Eq. (4) substituting  $L_m$  with  $L_e = -40.5a_0$ . This predicts the  $K_3$  coefficient to be two orders of magnitude smaller than the values measured at 850.1G. This is well below our resolution limit for the highest achievable densities set by collisions with residual atoms from vacuum. Thus from our data, we can only extract the upper limit for  $L_e$  at 575.9G,  $|L_e| < 100a_0$ , which is consistent with the predicted general trend of being smaller than the one at 850.1G.

In conclusion we show a surprisingly well-behaved three-body recombination rate at vanishing two-body scattering length. We identify that the only relevant parameters to define the three-body recombination rates in this limit are  $a$  and  $R_e$ , which together define the next non-vanishing coefficient in the two-body scattering phase shift. It is interesting to extend our studies to other atomic species. Feshbach resonances in  $^7\text{Li}$  are of intermediate character which is not the case for  $^{133}\text{Cs}$  atoms. Therefore a similar study for  $^{133}\text{Cs}$  and  $^{39}\text{K}$  would be interesting to complete the picture of a concise description of three-body recombination at a zero-crossing. It is also interesting to note that  $L'_e = 0$  at 744.15G. We thus predict that the three-body recombination rate will reach its minimum at this magnetic field. It might be an interesting region for a Bose-Einstein condensate whose lifetime should be maximized there. Counter-intuitively, it does not occur at zero scattering length. Finally, we note that the new length,  $L'_e$ , may play an important role in the effective range corrections to the lowest energy level in the Efimov spectrum.

Note that energy dependence of three-body recombinations were reported in the vicinity of a narrow Feshbach resonance in a two-component Fermi gas [24]. However, direct three-body recombination in such a mixture is forbidden and it is mediated through collisions of closed channel molecules with free atoms. This mechanism might become relevant for three-body recombination in Bose gases for extremely narrow Feshbach resonances.

*Note:* While finalizing this manuscript we became aware of a recently developed theory that strongly supports our findings [25].

L. K. and O. M. acknowledge fruitful discussions with C. H. Greene. This research was supported by grants from the United States-Israel Binational Science Foundation (BSF) and the Israel Science Foundation (ISF), Jerusalem, Israel.

- 
- [1] L. D. Faddeev and S. Merkuriev, *Quantum Scattering Theory for Several Particle Systems* (Springer, 1993).  
 [2] C. Chin, R. Grimm, P. Julienne, and E. Tiesinga, Rev. Mod. Phys. **82**, 1225 (2010).

- [3] E. Braaten and H.-W. Hammer, Phys. Rep. **428**, 259 (2006).  
 [4] Y. Wang, J. P. D'Incao, and B. D. Esry, Adv. At. Mol. Opt. Phys. **62**, 1 (2013).



- [5] J. Wang, J. P. D’Incao, B. D. Esry, and C. H. Greene, Phys. Rev. Lett. **108**, 263001 (2012).
- [6] P. Naidon, S. Endo, and M. Ueda, arXiv:1208.3912.
- [7] D. S. Petrov, Phys. Rev. Lett. **93**, 143201 (2004).
- [8] M. Jona-Lasinio and L. Pricoupenko, Phys. Rev. Lett. **104**, 023201 (2010).
- [9] L. Pricoupenko and M. Jona-Lasinio, Phys. Rev. A **84**, 062712 (2011).
- [10] F. Ferlaino, A. Zenesini, M. Berninger, B. Huang, H.-C. Nägerl, and R. Grimm, Few-Body Syst. **51**, 113 (2011).
- [11] R. J. Wild, P. Makotyn, J. M. Pino, E. A. Cornell, and D. S. Jin, Phys. Rev. Lett. **108**, 145305 (2012).
- [12] B. S. Rem, A. T. Grier, I. Ferrier-Barbut, U. Eismann, T. Langen, N. Navon, L. Khaykovich, F. Werner, D. S. Petrov, F. Chevy, et al., Phys. Rev. Lett. **110**, 163202 (2013).
- [13] S. Roy, M. Landini, A. Trenkwalder, G. Semeghini, G. Spagnolli, A. Simoni, M. Fattori, M. Inguscio, and G. Modugno, Phys. Rev. Lett. **111**, 053202 (2013).
- [14] B. Huang, L. A. Sidorenkov, R. Grimm, and J. M. Hudson, arXiv:1402.6161.
- [15] S.-K. Tung, K. Jiménez-García, J. Johansen, C. Parker, and C. Chin, arXiv:1402.5943.
- [16] R. Pires, J. Ulmanis, S. Häfner, M. Repp, A. Arias, E. D. Kuhnle, and M. Weidemüller, arXiv:1403.7246.
- [17] J. R. Taylor, *Scattering theory* (John Wiley and Sons, New York, 1972).
- [18] N. Gross, Z. Shotan, O. Machtey, S. Kokkelmans, and L. Khaykovich, C.R. Physique **12**, 4 (2011).
- [19] N. Gross, Z. Shotan, S. Kokkelmans, and L. Khaykovich, Phys. Rev. Lett. **103**, 163202 (2009).
- [20] N. Gross and L. Khaykovich, Phys. Rev. A **77**, 023604 (2008).
- [21] K. M. O’Hara, M. E. Gehm, S. R. Granade, and J. E. Thomas, Phys. Rev. A **64**, 051403(R) (2001).
- [22] T. Weber, J. Herbig, M. Mark, H.-C. Nägerl, and R. Grimm, Phys. Rev. Lett. **91**, 123201 (2003).
- [23] N. Gross, Z. Shotan, S. Kokkelmans, and L. Khaykovich, Phys. Rev. Lett. **105**, 103203 (2010).
- [24] E. L. Hazlett, Y. Zhang, R. W. Stites, and K. M. O’Hara, Phys. Rev. Lett. **108**, 045304 (2012).
- [25] Y. Wang and P. S. Julienne, arXiv:1404.0483.
- [26] S. Kokkelmans, arXiv:1401.2945.
- [27] For an isolated Feshbach resonance, it can be shown that  $V_e = (R^* a_{bg}^2 - r_{vdW}^3/3)$  exactly when  $a = 0$  [26], where  $a_{bg}$  is the background scattering length and  $R^*$  is inversely proportional to the width of the resonance. However, for overlapping resonances, as is the case in  $^7\text{Li}$ , the analytic expression for the effective length is more involved and will be subject of a future publication. Instead, we utilize here numerical values for  $L_e$  resulting from a coupled-channels calculation.
- [28] See Supplemental Material for details on evaporation cooling model.

## Supplemental Material

### Appendix A: Model of the evaporation cooling

The energy evolution in the time dependent optical dipole trap can be expressed as follows [S1]:

$$\frac{dE}{dt} = (\eta + \tilde{\kappa}) k_B T \frac{dN}{dt} + \frac{1}{U} \frac{dU}{dt} \frac{E}{2}, \quad (\text{S1})$$

where  $\eta = \epsilon_c/k_B T(0)$  is the truncation parameter with  $\epsilon_c$  being the truncation energy and  $\tilde{\kappa}$  stands for the energy carried away by the evaporated atom in addition to  $\epsilon_c$ . In an harmonic trap,  $\tilde{\kappa}$  can be evaluated analytically [S2]:

$$\tilde{\kappa} = \frac{1 - P(5, \eta)/P(3, \eta)}{\eta - 4P(4, \eta)/P(3, \eta)}, \quad (\text{S2})$$

where  $P(x, \eta)$  is the incomplete  $\Gamma$  function.

The first part in the right hand of Eq. (S1) is responsible for evaporation cooling. The second part describes the adiabatic cooling due to weakening of the optical dipole potential.

The potential depth is reduced exponentially in time:

$$U(t) = U_0 \exp\left(-\frac{t}{\tau}\right), \quad (\text{S3})$$

with the time constant  $\tau$  defined by the ratio of initial and final values of the potential depth:

$$\tau = \frac{t}{\ln\left(\frac{U_0}{U_f}\right)}. \quad (\text{S4})$$

Accordingly, the oscillation frequency in the trap reduces as:  $\bar{\omega}^2(t) = \bar{\omega}_0^2 \exp(-t/\tau)$  with  $\bar{\omega}_0 = (\omega_{r,0}^2 \omega_{z,0})^{1/3}$  being the geometric mean of the initial oscillation frequencies.

The atom number rate equation due to evaporation is:

$$\frac{dN}{dt} = -\Gamma_{ev} N, \quad (\text{S5})$$

where  $\Gamma_{ev} = \Gamma_{el} \xi_{ev}$ .  $\Gamma_{el} = n_0 \sigma(k) \bar{v}$  is the two-body elastic collision rate with  $n_0$  being the peak atomic density,  $\bar{v} = \sqrt{\frac{8}{\pi} \frac{k_B T}{m}}$  is the mean velocity of atoms at temperature  $T$  and  $\sigma(k)$  is the two-body collisional cross-section defined in Eq. (3) of the main text with the relative momentum  $k = \sqrt{\frac{m k_B T}{\hbar^2}}$ . In the harmonic trap the peak density can be related to  $\bar{\omega}$ ,  $T$  and the total number of atoms  $N$ :  $n_0 = N \left(\frac{m \bar{\omega}^2}{2 k_B T \pi}\right)^{3/2}$ . The evaporation efficiency  $\xi_{ev} = \left(\frac{V_{ev}}{V_e}\right) e^{-\eta}$  contains the ratio between the effective volume for elastic collisions leading to evaporation  $V_{ev}$  and the single atom volume  $V_e$  [S2]:

$$\frac{V_{ev}}{V_e} = \eta - 4 \frac{P(4, \eta)}{P(3, \eta)}. \quad (\text{S6})$$

Taking all these factors into account we can express Eq. (S5) in the final form:

$$\frac{dN}{dt} = -\gamma_1 (-a + \gamma_2 T)^2 \frac{N^2}{T} \exp\left(-\frac{3t}{2\tau}\right), \quad (\text{S7})$$

where, considering constant  $\eta$  and  $\sigma(k)$  to the lowest order in  $k$ ,

$$\gamma_1 = \xi_{ev} \frac{m\bar{\omega}_0^3}{\pi k_B}, \quad (\text{S8})$$

$$\gamma_2 = L_e^3 \frac{mk_B}{\hbar^2}. \quad (\text{S9})$$

In the harmonic trap the average energy per atom is  $E = 3k_bTN$ . From the time-derivative of this equation,

combined with Eqs. (S1) and (S5), we obtain:

$$\frac{dT}{dt} = -\frac{T}{3} \left( \Gamma_{ev} (\eta + \tilde{\kappa} - 3) + \frac{3}{2\tau} \right). \quad (\text{S10})$$

Finally, by substituting the expression for  $\Gamma_{ev}$ , we arrive at

$$\frac{dT}{dt} = -\frac{T}{3} \left( \gamma_3 (-a + \gamma_2 T)^2 \frac{N}{T} \exp\left(-\frac{3t}{2\tau}\right) + \frac{3}{2\tau} \right), \quad (\text{S11})$$

where  $\gamma_3 = \gamma_1 (\eta + \tilde{\kappa} - 3)$ .

Eqs. (S7) and (S11) form a set of two coupled differential equations describing evaporation cooling dynamics. Their solution is represented in Fig. 2 of the main text.

- 
- [S1] K. M. O'Hara, M. E. Gehm, S. R. Granade, and J. E. Thomas, Phys. Rev. A **64**, 051403(R) 2001.  
[S2] O. J. Luiten, M. W. Reynolds and J. T. M. Walraven,

Phys. Rev. A **53**, 381 1996.